

Cartilaginous Extracellular Matrix-Modified Chitosan Hydrogels for Cartilage Tissue Engineering

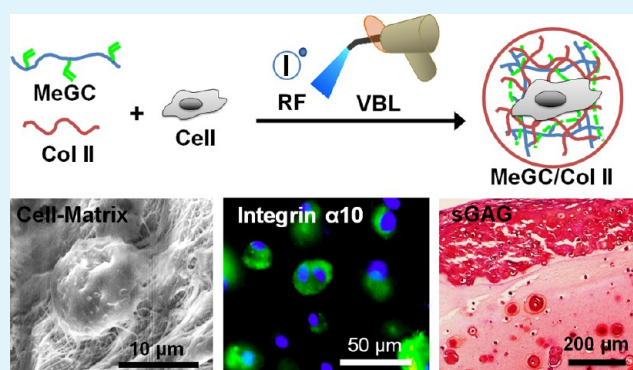
Bogyu Choi,[†] Soyon Kim,[‡] Brian Lin,[†] Benjamin M. Wu,^{†,‡} and Min Lee^{*,†,‡}

[†]Division of Advanced Prosthodontics, [‡]Department of Bioengineering, University of California, Los Angeles, Los Angeles, California 90095, United States

Supporting Information

ABSTRACT: Cartilaginous extracellular matrix (ECM) components such as type-II collagen (Col II) and chondroitin sulfate (CS) play a crucial role in chondrogenesis. However, direct clinical use of natural Col II or CS as scaffolds for cartilage tissue engineering is limited by their instability and rapid enzymatic degradation. Here, we investigate the incorporation of Col II and CS into injectable chitosan hydrogels designed to gel upon initiation by exposure to visible blue light (VBL) in the presence of riboflavin. Unmodified chitosan hydrogel supported proliferation and deposition of cartilaginous ECM by encapsulated chondrocytes and mesenchymal stem cells. The incorporation of native Col II or CS into chitosan hydrogels further increased chondrogenesis. The incorporation of Col II, in particular, was found to be responsible for the enhanced cellular condensation and chondrogenesis observed in modified hydrogels. This was mediated by integrin $\alpha 10$ binding to Col II, increasing cell–matrix adhesion. These findings demonstrate the potential of cartilage ECM-modified chitosan hydrogels as biomaterials to promote cartilage regeneration.

KEYWORDS: type-II collagen, chondroitin sulfate, chitosan, photopolymerization, hydrogels, cartilage tissue engineering



1. INTRODUCTION

Regeneration of damaged articular cartilage is clinically challenging because of its limited ability for self-repair.^{1–3} Therefore, tissue engineering approaches are being investigated and are showing promise for the treatment of degenerative joint diseases such as osteoarthritis. In articular cartilage, chondrocytes are surrounded by a highly hydrated extracellular matrix (ECM) consisting of type-II collagen (Col II), proteoglycans, and various other proteins.^{4,5} Hydrogels are cross-linked polymer networks that swell in aqueous solution and present a unique opportunity for cartilage regeneration by introducing chondrocytes or their precursors into a physically controllable environment similar to articular cartilage, which allows the efficient transport of nutrients and biological molecules.⁶ In addition, hydrogels can be formed in situ through minimally invasive administration to deliver therapeutic molecules or progenitor cells to defective or diseased tissues.⁶

During chondrogenesis, mesenchymal stem cells (MSCs) produce a variety of glycosaminoglycans (GAGs) and fibrous ECM proteins such as collagens (Col), especially Col II, which is the main structural protein in articular cartilage. Chondroitin sulfate (CS) is a sulfated GAG (sGAG), which forms proteoglycans trapped within the Col II fibril framework. These molecules not only play a crucial role in providing articular cartilage with mechanical strength but also are proven

to support cell proliferation and maintain the chondrogenic phenotype.^{7–9} Previous studies have demonstrated that Col II or CS enhance proliferation and deposition of cartilaginous ECM by chondrocytes or MSCs in cartilage tissue engineering.^{10–14} Furthermore, Col has been shown to induce cell aggregation and subsequent chondrogenic differentiation through integrin-mediated cell adhesion on its triple helical fibers.^{12,15,16}

Although they have critical roles in the formation of cartilage tissue, use of Col or CS alone is limited for cartilage tissue engineering applications due to their high degree of water solubility and rapid enzymatic degradation.^{11,17,18} Chemical cross-linking can enhance the physical stability of Col or CS, but this is at the expense of biological activity of the therapeutic agents and living cells to be encapsulated. It has been shown that cross-linking of Col with glutaraldehyde, a common cross-linking agent, caused apoptosis of human osteoblasts that was associated with poor cell attachment and spreading, indicating glutaraldehyde toxicity.¹⁹ Similar observations of in vitro cytotoxicity have been reported in dermal sheep Col cross-linked with hexamethylene diisocyanate.²⁰ Although Col can spontaneously gel by self-assembly without chemical mod-

Received: August 24, 2014

Accepted: October 31, 2014

Published: October 31, 2014

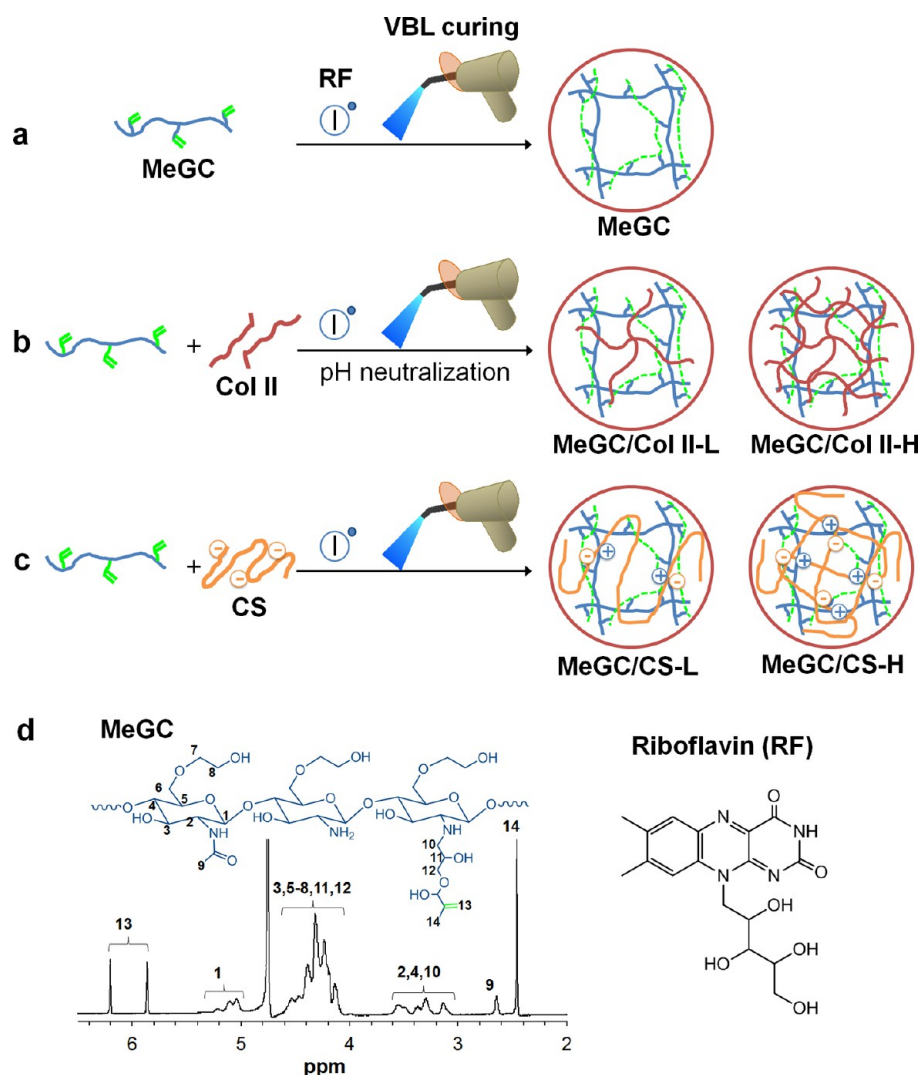


Figure 1. Design of VBL cross-linkable chitosan/ECM composite hydrogels. (a) Chitosan hydrogel is prepared by cross-linking of MeGC via VBL irradiation with RF. (b) Mixture of MeGC with Col II and RF is pH neutralized for initiating Col II gelation and followed by VBL-cross-linking to form a hydrogel (MeGC/Col II). Fibrous structure of hydrogel can be varied in a Col II concentration dependent manner. (c) Ionically interacted MeGC and CS is cross-linked using VBL irradiation with RF (MeGC/CS). (d) ¹H NMR spectra and structures of MeGC in D₂O. Structure of RF.

ifications, physically cross-linked gels often show low dimensional stability with significant shrinkage and degradation in culture.^{17,18}

We have previously developed injectable hydrogels using photopolymerizable chitosan (methacrylated glycol chitosan; MeGC) and riboflavin (RF; vitamin B2) as an aqueous initiator that allows gelation in situ upon exposure to visible blue light (VBL).²¹ This gelation system is prepared under very mild conditions (room temperature, physiological pH, naturally derived water-soluble initiator, and rapid curing), reducing potential adverse effects associated with UV irradiation and toxic initiators. Chitosan, a polysaccharide derived from naturally occurring chitin, is widely used in tissue engineering applications.^{22–28} In particular, it is an attractive matrix to facilitate cartilage tissue repair because of its biocompatibility and structural similarity to GAGs found in articular cartilage. Moreover, the free amino groups in chitosan allow the formation of stable polyelectrolyte complex hydrogels with many anionic molecules in tissue ECM such as Col and CS.

Here, we report the use of injectable formulations of natural cartilaginous ECM (Col II and CS) enhanced by VBL-inducible

chitosan hydrogels (MeGC/Col II and MeGC/CS) for potential use in cartilage regeneration. Specifically, a hydrogel was formed by mixing solutions of unpolymerized MeGC with Col II or CS followed by VBL-cross-linking in the presence of RF (Figure 1). The naturally derived hydrogel matrix studied here also contains type-I Col (Col I), the main protein found in connective tissue, and denatured Col II (dCol II) allowing further investigation of the effects of matrix surface specificity and fibrous Col structure on cellular responses. The feasibility of these hydrogel systems to support chondrogenic differentiation was investigated by encapsulating chondrocytes and MSCs in vitro.

2. EXPERIMENTAL SECTION

2.1. Photopolymerizable Hydrogel Preparation. VBL inducible MeGC was prepared as previously described.²¹ Briefly, glycidyl methacrylate (Sigma-Aldrich, St. Louis, MO) was added to a 2% w/v glycol chitosan (GC; Sigma-Aldrich; ~500 kDa) aqueous solution (pH 9.0) with 1:1 molar ratio of glycidyl methacrylate to the primary amino groups in chitosan and allowed to react for 36 h with gentle shaking at room temperature. The reaction mixture was then neutralized, dialyzed against water using a membrane with a 50 kDa molecular

weight cutoff for 15 h, and lyophilized. The degree of deacetylation of GC and degree of substitution of MeGC were calculated via ^1H NMR spectra. We previously enhanced the ability of the hydrogel to promote tissue regeneration by adding Col I or hyaluronic acid at concentrations of 0.1–1.0% into the hydrogel.^{21,29} Col II (Sigma-Aldrich, from chicken sternal cartilage) is insoluble in water (10 mg/mL in 0.01 M acetic acid), and CS (Sigma-Aldrich) concentrations above 1% w/v reduced the modulus of the cross-linked hydrogel. Based on these findings, the final concentrations of 0.2 and 0.4% w/v for Col II and 0.5 and 1% w/v for CS were chosen for the current studies. The experimental groups are specified in Table 1. Briefly, the

Table 1. List of Experimental Groups

group	concentration of MeGC (% w/v)	concentration of Col II (% w/v)	concentration of CS (% w/v)
MeGC	2	0	0
MeGC/ Col II-L	2	0.2	0
MeGC/ Col II-H	2	0.4	0
MeGC/ CS-L	2	0	0.5
MeGC/ CS-H	2	0	1.0

MeGC (2% w/v) composite solutions containing 0.2% w/v of Col II (MeGC/Col II-L), 0.4% w/v of Col II (MeGC/Col II-H), 0.5% w/v of CS (MeGC/CS-L), or 1% w/v of CS (MeGC/CS-H) were prepared by mixing stock solutions of MeGC (4% w/v in phosphate buffered saline, PBS) with Col II (1.0% w/v, in 0.05% acetic acid) or CS (2% w/v in PBS). MeGC solutions (2% w/v) without additives were prepared by diluting the 4% w/v MeGC in PBS. The hydrogel was formed by exposing 40 μL of the solution to visible blue light (400–500 nm, 500–600 mW/cm^2 ; Bisco Inc., Schaumburg, IL) in the presence of RF (final concentration 6 μM), as a photoinitiator.

2.2. Hydrogel Characterization. The gelation time of the chitosan and chitosan/ECM composite solutions under VBL irradiation with different concentrations of RF (1.5, 3, 6, 12, and 24 μM) was investigated by a test tube tilting method as previously described ($n = 3$).²⁹ The compressive modulus of hydrogels (400 μL with 6 μM RF; 40 s VBL-irradiation in 48-well plates) was measured via an indentation experiment with an Instron electromechanical testing machine (Instron, Model 5564, Norwood, MA) using a flat-ended indenter 3 mm in diameter and calculated as described previously using a Poisson's ratio of 0.25 ($n = 3$).²⁵ To determine in vitro gel degradation, the cross-linked hydrogels were incubated in 3 mL of PBS with or without lysozyme (Sigma-Aldrich, 2 mg/mL)^{27,30,31} at 37 °C for up to 42 days. The lysozyme solution was replaced twice a week. At various time-points, the incubating media was removed and the wet weight of remaining gels was measured after gentle blotting without drying hydrogels. The amount of remaining gel was expressed as a percentage of the initial wet mass of the gel ($n = 3$). The interior morphology and cell–matrix interactions of the photo-cross-linked hydrogels were observed using scanning electron microscopy (SEM; Nova NanoSEM230, FEI, Hillsboro, OR). Prior to SEM analysis, the hydrogels were fixed in 2.5% glutaraldehyde (Polysciences, Warrington, PA) and then observed in low vacuum mode.

2.3. Cell Isolation and in Vitro 3D Culture. All studies involving animals were carried out using protocols approved by the UCLA Chancellor's Animal Research Committee (ARC) and were in accordance with National Institutes of Health regulations on the Care and Use of Laboratory Animals. Chondrocytes were isolated from the knees of 3 month old male New Zealand white rabbits (Charles River Laboratories, Wilmington, MA), as rabbit chondrocytes were shown to proliferate and deposit cartilaginous ECM in our previous study using alginate gels.³² The harvested cells were expanded in the culture medium consisting of Dulbecco's modified Eagle's medium (DMEM, Cellgro, Manassas, VA) with 10% fetal bovine

serum (Gibco, Carlsbad, CA), 100 U/ml penicillin (Cellgro), and 100 $\mu\text{g}/\text{mL}$ streptomycin (Cellgro) at 37 °C in a 5% CO_2 humidified atmosphere. Chondrocytes (passage 3) suspended in polymer solution (40 μL at a density of 2×10^6 cells/mL) were exposed to VBL for 40 s in the presence of 6 μM RF and grown in culture media. To evaluate the capacity of the hydrogels to support chondrogenic differentiation of MSCs, adipose derived MSCs (ADSCs) were isolated from inguinal fat pads of 4–8 week old male C57BL/6 mice (Charles River Laboratories) as previously described, as these cells were able to differentiate into multiple mesenchymal lineages, including chondrogenic, osteogenic, and adipogenic lineages, in specific differentiation media in our previous study.³³ An ADSC-polymer suspension at a density of 10×10^6 cells/mL was VBL-cross-linked and cultured in standard MSC chondrogenic differentiation media, consisting of culture media plus ITS+ Premix supplement (BD Biosciences, Bedford, MA), 10 ng/mL TGF- β 1 (PeproTech, Rocky Hill, NJ), 100 nM dexamethasone, 40 $\mu\text{g}/\text{mL}$ L-proline, 1 mM sodium pyruvate, and 50 $\mu\text{g}/\text{mL}$ L-ascorbic acid 2-phosphate (all from Sigma-Aldrich).

2.4. Cell Proliferation, Viability, and Differentiation. The 3D cultured samples were analyzed for proliferation, viability, and differentiation. The proliferation of chondrocytes in hydrogels was assessed using a Quant-iT Picogreen dsDNA kit (Invitrogen, Carlsbad, CA) according to the manufacturer's protocol ($n = 3$). Viability of chondrocytes and ADSCs in hydrogels was determined using the Live/Dead assay kit (Invitrogen). Stained cells were observed using an Olympus IX71 microscope (Olympus, Tokyo, Japan). Accumulation of sGAG in hydrogel was measured using a 1,9-dimethyl-methylene blue (DMB, Sigma-Aldrich) assay and then further normalized to the dry weight of each sample.

2.5. Histological Analysis. For histology, cultured constructs were fixed in 10% neutral buffered formalin, embedded in paraffin, and sectioned at 5 μm . Sections were deparaffinized and stained with hematoxylin and eosin (H&E) to examine cellular distribution and morphology, safranin-O to assess sGAG, and immunohistochemistry to determine Col II production. For immunohistochemistry of accumulated Col II, sections were incubated with monoclonal anti-rabbit Col II (EMD Millipore, Billerica, MA). Antibody was detected using the SuperPicture polymer detection kit (Invitrogen). GAG and Col II accumulated area were relatively quantified by using NIH-ImageJ software (<http://rsb.info.nih.gov/ij/>) ($n = 3$).

2.6. Conformational Change of Col. To investigate the effects of Col conformation on chondrogenesis, Col II was denatured by heat treatment at 95 °C for 30 min as previously described.³⁴ The conformational change of Col II was determined by circular dichroism (CD) spectroscopy (J-715, JASCO, Tokyo, Japan) as previously described.³⁵ Because Col II forms a triple helical structure similar to Col I, CD spectra measurements were also performed for Col I (PureCol, Advanced Biomatrix, San Diego, CA).

2.7. Integrin Expression. To determine the effects of the conformational change of Col on integrin expression, ADSCs were encapsulated in MeGC hydrogels containing Col I, Col II, or dCol II at a density of 10×10^6 cells/mL as described above. ADSCs encapsulated in hydrogels were fixed after 24 h culture with 2% paraformaldehyde, permeabilized with 0.1% Triton X-100, and blocked with 2 mg/mL BSA. Hydrogels were incubated overnight with the mixture of primary antibodies to integrin α 3 (rabbit anti-mouse integrin α 3, Santa Cruz, CA; Dallas, TX) and integrin α 10 (goat anti-mouse integrin α 10, Santa Cruz) at 4 °C, washed, and then incubated with mixture of secondary antibodies (donkey anti-rabbit IgG-R and donkey anti-goat IgG-fluorescein isothiocyanate (FITC) from Santa Cruz). Nuclei were stained with 4',6-diamidino-2-phenylindole (DAPI) and images were obtained using an Olympus IX71 microscope.

2.8. Statistical Analysis. Sol–gel transition, hydrogel degradation, and DNA or sGAG content data were analyzed by two-way analysis of variances (ANOVA), and all other data were analyzed by one-way ANOVA followed by Turkey's post hoc test. A value of $p < 0.05$ was considered as significant.

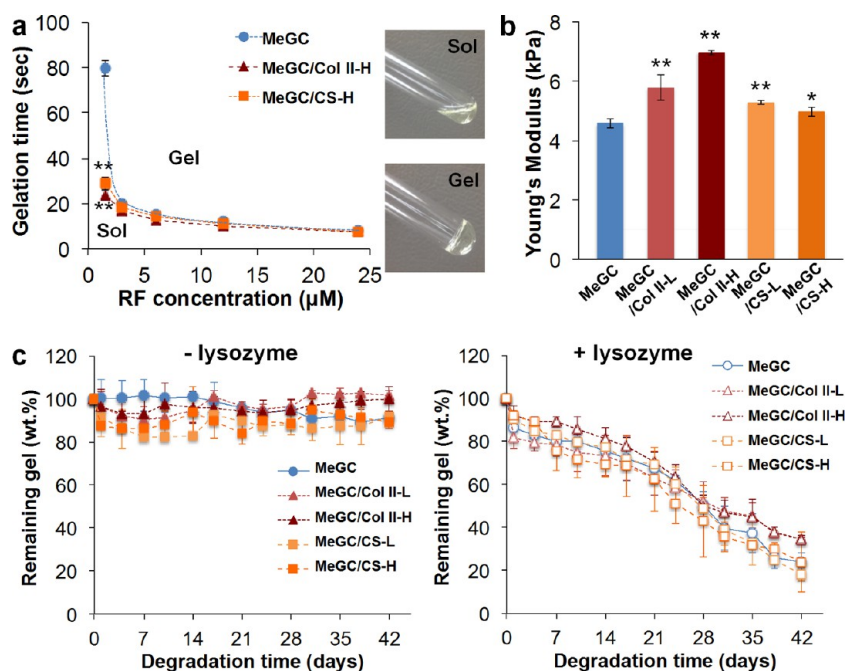


Figure 2. Hydrogel characterization. (a) Gelation time of chitosan (MeGC) and chitosan/ECM composite (MeGC/Col II-H and MeGC/CS-H) solutions as a function of RF concentration determined by test tube tilting method ($n = 3$; $**p < 0.01$ compared with MeGC). (b) Mechanical strength of hydrogels (MeGC, MeGC/Col II-L (0.2% w/v of Col II), MeGC/Col II-H (0.4% w/v of Col II), MeGC/CS-L (0.5% w/v of CS), and MeGC/CS-H (1.0% w/v of CS)). (c) In vitro mass loss of hydrogels in PBS without or with lysozyme ($n = 3$).

3. RESULTS AND DISCUSSION

3.1. Sol–Gel Transition of Hydrogels. MeGC was prepared via methacrylation to the GC, as described in section 2.1. The degree of substitution of methacrylate to the GC was 26%, as determined via ^1H NMR (Figure 1d). Fast gelation is desired for in situ forming hydrogels to rapidly entrap cells and bioactive molecules at a complex defective site with good integration with surrounding tissues.³⁶ The sol-to-gel transition time was determined as a function of RF concentration (Figure 2a). The MeGC solution with 1.5 μM of RF showed sol–gel transition after 80 ± 4 s of irradiation. The sol-to-gel transition time of MeGC rapidly decreased from 80 ± 4 to 20 ± 2 s with increasing RF concentration from 1.5 μM to 3 μM , whereas a further increase of RF concentration up to 24 μM had little influence on the transition time. Addition of Col II (0.4% w/v) or CS (1.0% w/v) significantly decreased the gelation time from 80 ± 4 to 24 ± 2 or 29 ± 3 s, respectively, with 1.5 μM RF (MeGC/Col II-H or MeGC/CS-H in Figure 2a). These VBL/RF-initiated chitosan hydrogels showed relatively faster gelation compared to UV/lithium acylphosphinate or Irgacure 2959-initiated hydrogel systems that required a longer irradiation time of 180 s with polyethylene glycol (PEG) or MeGC-based hydrogels.^{37–39} Because RF concentrations above 3 μM did not significantly change the gelation time of hydrogels ($p > 0.1$) and gelation occurred within 20 s, a slightly higher RF concentration (6 μM) and irradiation time (40 s) were investigated in further studies.

3.2. Mechanical Properties of Hydrogels. The mechanical strength of hydrogels was characterized in the presence or absence of Col II or CS with 6 μM of RF and 40 s of VBL irradiation (Figure 2b). Addition of Col II significantly increased the compressive modulus of MeGC from 4.6 to 5.8 or 7.0 kPa at Col II content of 0.2% w/v (MeGC/Col II-L) or 0.4% w/v (MeGC/Col II-H), respectively. The enhanced mechanical strength of the composite hydrogels can be

attributed to the formation of an interpenetrating network (IPN) by Col II in the cross-linked MeGC network. It was previously demonstrated that mechanical strength is enhanced in semi-IPN and IPN hydrogels created by agarose and photo-cross-linkable PEG,⁴⁰ or Col and photo-cross-linkable hyaluronic acid (HA).⁴¹ It is possible that the radical polymerization can cause cross-linking of thiol moieties in proteins such as cysteine amino acids; however, this effect is unlikely in the MeGC/Col II hydrogels, given the lack of cysteine residues in Col II.^{42,43} Addition of CS also enhanced the modulus of MeGC from 4.6 to 5.3 or 5.0 kPa at a CS content of 0.5% w/v (MeGC/CS-L) or 1.0% w/v (MeGC/CS-H). The observed enhanced mechanical modulus may be attributed to the ionic interaction between MeGC and CS. In previous studies, similar mechanical effects mediated by ionic interactions were reported between cross-linked MeGC and HA in composite hydrogels²⁹ or in chitosan-coated alginate filaments.⁴⁴ Although the observed mechanical properties of the hydrogels are orders of magnitude lower than those of cartilage (4–19 MPa),⁴⁵ it is expected that implanted cells will generate new cartilage tissue as the hydrogel degrades, which in turn will ultimately provide mechanical support.

3.3. Degradation of Hydrogels. Tissue engineering scaffolds must be designed to degrade, to allow subsequent tissue regeneration or the release of encapsulated bioactive molecules. Chitosan is enzymatically degraded by lysozyme present in the human cartilage ECM³⁰ and in certain body fluids.^{46–48} Lysozyme-specific degradation has been shown with various chitosan-based hydrogels or scaffolds.^{21,25,27,29} To examine whether photo-cross-linked chitosan is degradable by lysozyme and whether addition of Col II or CS affects the degradation behavior of hydrogels, MeGC and ECM-modified chitosan hydrogels were incubated in PBS with or without lysozyme at 37 $^\circ\text{C}$ for up to 42 days (Figure 2c). Lysozyme was used at a concentration of 2 mg/mL to mimic the physiological

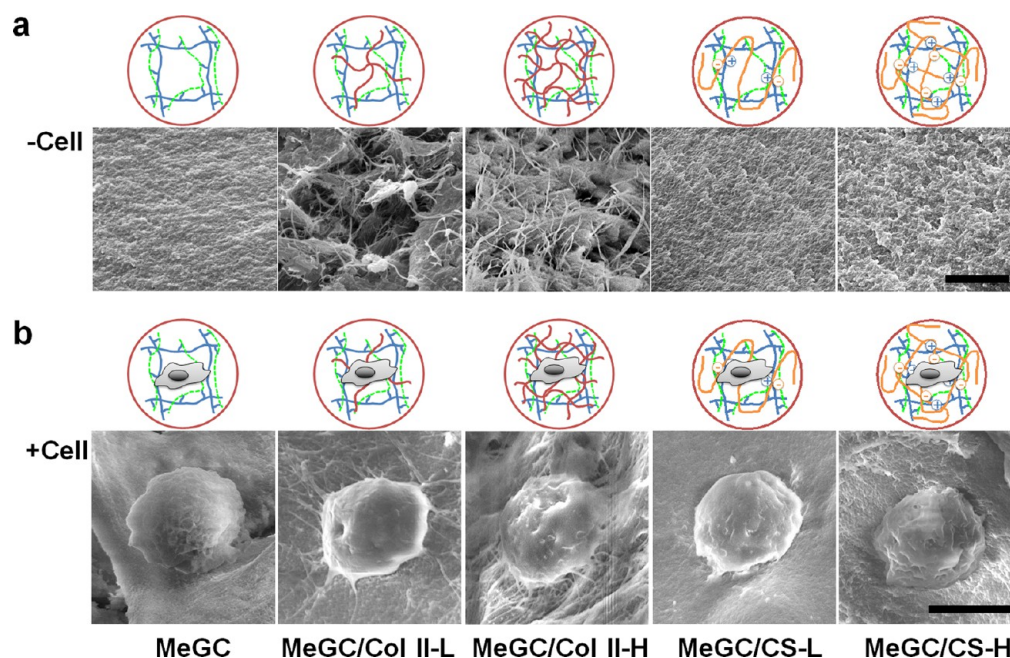


Figure 3. SEM images of hydrogels. (a) Interior morphology of hydrogels. The scale bar is 5 μm . (b) Cell adhesion to the hydrogels. The scale bar is 10 μm .

conditions in cartilage (lysozyme concentration range in human cartilage: 0.80–3.03 mg/g).³⁰ As expected, photo-cross-linked MeGC was stable in the absence of lysozyme during the incubation (remaining mass: 91%). In the presence of lysozyme, a significant time-dependent loss of MeGC mass was observed (remaining mass: 34%). Addition of Col II or CS did not significantly affect the degradation behavior of hydrogels and showed lysozyme-dependent degradation similar to unmodified MeGC. Specifically, there was no significant mass loss of hydrogels in PBS for up to 42 days (Figure 2c left), indicating that the incorporated ECM molecules remained in the hydrogels during the incubation period. Nonetheless, the ECM molecules can quickly diffuse out of the hydrogels, as the additives are not covalently incorporated to the gels. Thus, we have performed release studies to measure the Col II or CS contents in incubating solutions using biochemical assays. Approximately 3.2% or 6.4% of the initially loaded Col II or CS was released from the hydrogels during the first 4 days followed by a plateau, indicating that the incorporated ECM molecules are retained well in the hydrogels during incubation (Figure S1, Supporting Information).

3.4. Microstructure of Hydrogels and Cell-Matrix Interaction. The interior morphology of the hydrogels was examined using SEM (Figure 3a). The cross-sectional SEM images revealed that the surface of MeGC was smooth, whereas fibrous nanostructures were observed throughout the MeGC/Col II in a Col II-dose-dependent manner (MeGC/Col II-L and MeGC/Col II-H in Figure 3a). In MeGC/CS, the surface was relatively rough compared with MeGC but fibrous nanostructures were not observed.

Cell–matrix interaction was investigated by encapsulating chondrocytes in hydrogels and culturing them for 1 day (Figure 3b). Cross-sectional SEM images showed that chondrocytes remained rounded without interacting with the MeGC matrix. In contrast, cells encapsulated in MeGC/Col II appeared to form projections and interact with the surrounding hydrogel matrix. However, the cells maintained a round shape character-

istic of chondrocytes and no spreading was observed, indicating that MeGC/Col II supported their differentiated phenotype. Chondrocytes in MeGC/CS formed fewer projections compared to those in MeGC/Col II.

3.5. Viability and Proliferation of Chondrocytes in Hydrogels. To evaluate the effects of hydrogel composition on the behaviors of fully differentiated chondrocytes, we encapsulated chondrocytes within the hydrogels and characterized their change of morphology, viability, and DNA content. During chondrogenesis, undifferentiated mesenchymal cells condense and produce various ECM components, indicating that cell–cell and cell–matrix interactions are important steps in early cartilage formation.⁴⁹ Chondrocytes formed cellular aggregates during 6 weeks of culture in MeGC (Figure 4a), indicating that MeGC supported chondrogenic differentiation. Incorporation of Col II or CS in MeGC significantly increased the number and size of cell aggregates in a dose-dependent manner. In particular, cell clusters become evident in MeGC/Col II-H by 3 weeks and continued to increase in size over time. Live/Dead staining showed a high level of viability of encapsulated chondrocytes over the 6 week culture period in all conditions (Figure 4b). Proliferation of chondrocytes in hydrogels was further studied by DNA quantification using a PicoGreen assay (Figure 4c). Addition of Col II to MeGC significantly increased DNA content compared to MeGC alone by day seven. Similar proliferative effects of Col II were previously observed in GAG or polycaprolactone scaffolds supplemented with Col II.^{11,13} The accumulation of sGAG in hydrogels was quantified using a DMB assay (Figure 4d). After 6 weeks in culture, significantly higher sGAG production was observed in composite hydrogels compared with MeGC, with the highest sGAG production in MeGC/Col II-H (4.6-fold higher compared to MeGC). It has been reported that Col II and CS provide favorable chondrogenic environments for MSCs and chondrocytes.^{10–14,50}

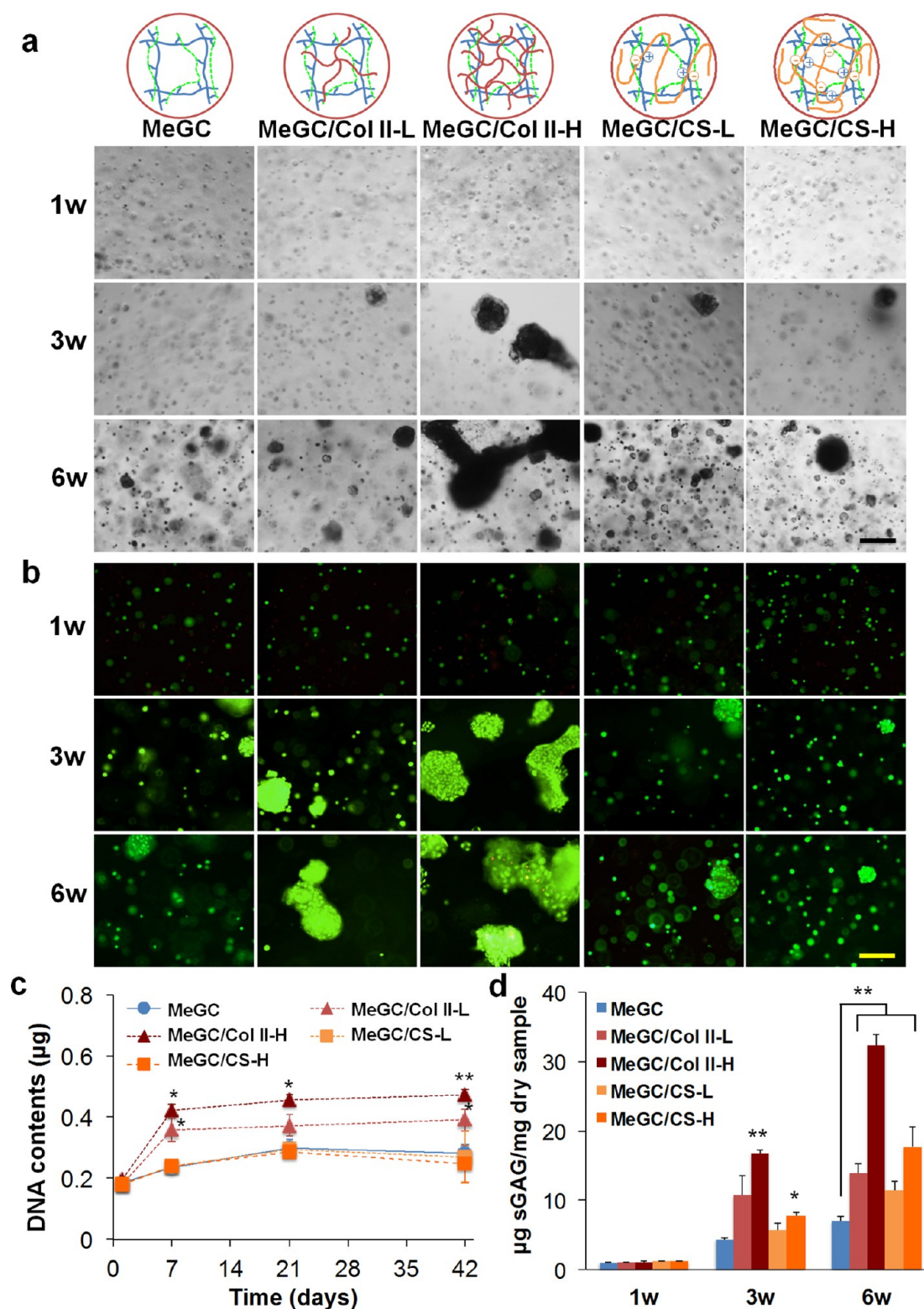


Figure 4. Culture of chondrocytes in hydrogels. (a) Morphological change and (b) viability of encapsulated chondrocytes in hydrogels after 6 weeks in culture. Cells are stained using a Live (green)/Dead (red) kit. The scale bar is $200 \mu\text{m}$. (c) Increase of DNA contents during culture period is correlated with cell proliferation, and this was analyzed using Picogreen assay ($n = 3$; $*p < 0.05$ and $**p < 0.01$ compared with MeGC). (d) Quantification of sGAG content as performed by DMB assay at 1, 3, and 6 weeks in culture and the value was then further normalized to the dry weight of each sample to determine chondrogenic potential of hydrogels ($n = 3$; $*p < 0.05$ and $**p < 0.01$ compared with MeGC).

3.6. Cartilaginous ECM Production in Hydrogels. The feasibility of MeGC/Col II and MeGC/CS to support chondrogenic differentiation was further investigated by histological examination. H&E staining revealed that encapsu-

lated chondrocytes maintained their characteristic round shape over the culture period in all experimental hydrogel groups (Figure 5a). Cell clusters were formed after 3 weeks in culture and continued to increase in number and size over time.

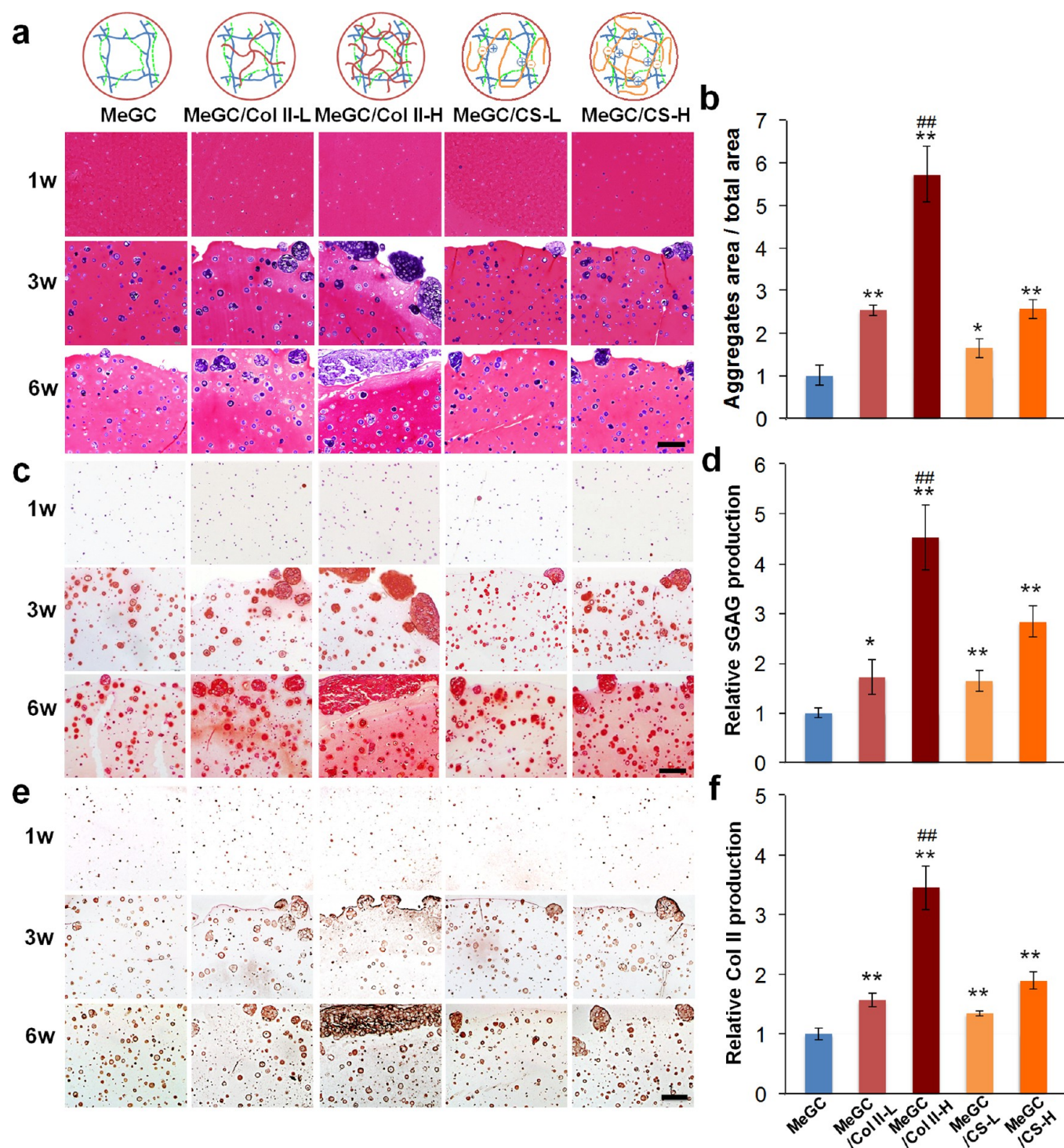


Figure 5. Histological analysis of 3D cultured chondrocytes in hydrogel systems during 6 week culture. Sections are stained with (a) H&E, (c) safranin-O (sGAG: orange red), and (e) immunohistochemical staining of Col II (brown) at 1, 3, and 6 weeks in culture. The scale bar is 200 μm . Aggregates area (b), production of sGAG (d), and production of Col II (f) at 6 weeks in culture are quantified by image analysis of staining samples using ImageJ and expressed as a fold-increase relative to pure MeGC groups ($n = 3$; * $p < 0.05$ and ** $p < 0.01$ compared with MeGC; ## $p < 0.01$ compared with other groups).

Addition of Col II or CS significantly increased the area of cell aggregates per unit gel area in a dose-dependent manner and significantly larger aggregates were formed in MeGC/Col II-H compared to any other experimental hydrogels (Figure 5b). The observed cellular aggregation is likely due to cell migration and merging in hydrogels rather than cell proliferation, since DNA content did not significantly increase after day seven

(Figure 4c). Other studies have also demonstrated that cellular aggregation could be due to migration and fusion of small clusters of cells.^{51,52} Cartilaginous ECM deposition was evaluated by immunohistochemistry for Col II and safranin-O staining to observe sGAG. Accumulation of sGAG increased over the culture period and positive safranin-O staining was observed immediately adjacent to chondroid cell clusters in

MeGC after 6 weeks (Figure 5c). In contrast, the region of safranin-O positive ECM extended into the hydrogel matrix surrounding the cell clusters in MeGC/Col II and MeGC/CS after 6 weeks in culture, indicating increased sGAG accumulation. In particular, MeGC/Col II-H showed highly intense safranin-O staining throughout the hydrogel matrix as well as around cellular aggregates. Relative quantitation of safranin-O staining showed 4.5-fold higher sGAG production in MeGC/Col II-H compared to MeGC (Figure 5d), which is similar to the results from the DMB assay (Figure 4d). Similarly to sGAG accumulation trends, Col II production from encapsulated cells increased over time and highly intense Col II staining was observed in composite hydrogels compared with MeGC (Figure 5e). Immunostaining showed Col II secretion increased as follows: MeGC < MeGC/CS-L < MeGC/Col II-L < MeGC/CS-H < MeGC/Col II-H after 6 weeks in culture. Col II production was 3.5-fold higher for MeGC/Col II-H compared to MeGC (Figure 5f). We also performed immunohistochemistry for Col types I and X, markers of immature and hypertrophic chondrocytes, respectively. Col types I and X were detected minimally in MeGC/Col II groups (Figure S2, Supporting Information), suggesting the presence of mature chondrocytes that are not hypertrophic in the hydrogels and a stable hyaline phenotype. Our results suggest that MeGC/Col II-H is the most promising chondrogenic matrix among the experimental groups examined here. Future studies will investigate the combined effects of Col II with CS, in particular, with a high Col II to CS ratio, given the high amount of Col II relative to CS in normal articular cartilage.⁵³

Histologic staining revealed a high cell cluster density in the outer region of the hydrogels, while the cluster density remained low in the interior region. The observed heterogeneous cell distribution in the hydrogels might be due to mass transport and nutrient exchange limitations whereby insufficient oxygen and soluble factors are transported to the interior regions of the hydrogels, resulting in cell death. Similar growth limitation of seeded cells was observed in tissue engineering 3D scaffolds in previous studies.^{54–59} More work is needed to address this issue. It has been shown that microchannel networks can be embedded within a cell-laden hydrogel using micro- and nanofluidic technologies to facilitate nutrient and metabolite diffusion in 3D tissue constructs.^{60,61}

Our previous studies demonstrated a 5- to 10-fold increase in gel modulus with increased irradiation from 40 s up to 300 s without compromising cell viability.^{21,29} We therefore further investigated the effect of hydrogel modulus on chondrogenesis. The compressive modulus of hydrogels significantly increased from approximately 4.6–7.0 to 10–14 kPa with an increase in irradiation time from 40 to 120 s (Figure 6a). However, increasing the hydrogel modulus led to significant reduction in sGAG secretion from chondrocytes encapsulated in the hydrogel (Figure 6b). This may be due to more highly cross-linked and stiffer hydrogels that suppressed matrix contraction or cellular migration, and subsequent reduction of the degree of cellular condensation and matrix synthesis.⁶² It is also possible that free radicals produced during photopolymerization have detrimental effects on encapsulated biomolecules, leading to DNA fragmentation, protein denaturation, and cell damage.⁶³ These results suggest that it will be critical to maintain a balance between initial mechanical strength and cellular differentiation for successful cartilage tissue regeneration.

3.7. Conformational Change of Different Col Types. Native Col consists of three polypeptide chains that self-

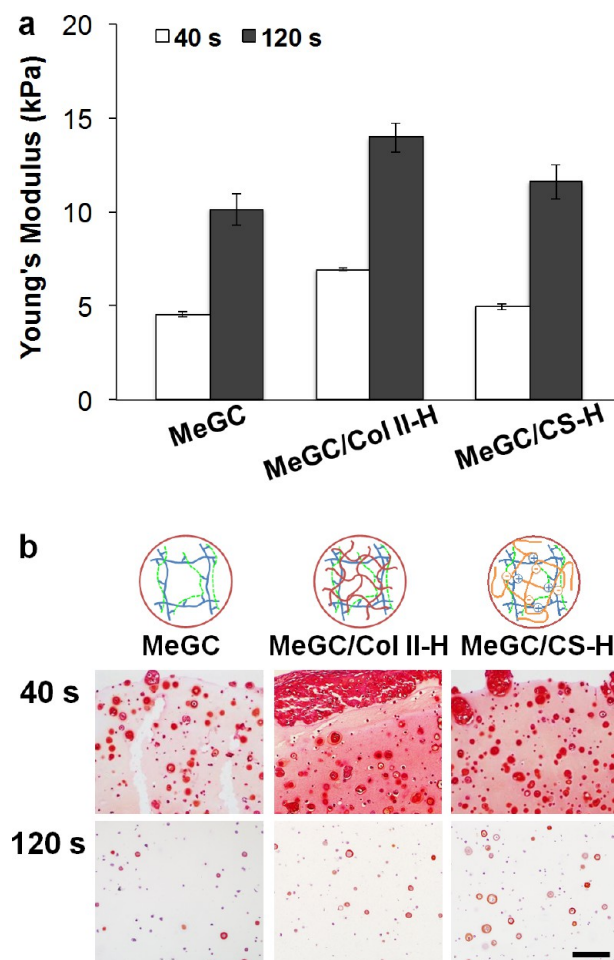


Figure 6. Effects of hydrogel modulus. (a) Mechanical strength of hydrogels with different VBL irradiation times (40 and 120 s). (b) Safranin-O staining for the sections of 3D cultured chondrocytes in the 40 and 120 s irradiated hydrogels after 6 weeks in culture. The scale bar is 200 μm .

assemble into a triple helix via periodic interchain hydrogen bonds. These unique triple helical structures of Col play important roles in tissue development and regeneration.¹⁶ The influence of triple helical structures on chondrogenesis was investigated by encapsulating ADCSs in dCol II with MeGC (MeGC/dCol II). We also evaluated the specificity of triple helical conformation on chondrogenesis by using Col I, the most abundant structural protein in connective tissue. CD spectra confirmed the triple helical structure of Col I and Col II, whereas dCol II lost the typical band for its helical structure, indicating that heat denaturation altered the structure of Col II from a triple helix to random coil (Figure 7a). Fourier transform infrared (FTIR) analysis confirmed the preservation of the triple helical structure of Col II after being incorporated into the hydrogel (Figure S3, Supporting Information). The amide I band (C=O stretching) for both pure Col II and composite MeGC/Col II hydrogels showed highly intense peaks at around 1656 cm^{-1} , which indicate an α -helical secondary structure.^{64–66} The amide A peaks (N—H stretching) for Col II and MeGC/Col II were found at around 3300 cm^{-1} , which was shifted to lower than typical free amide N—H stretching (3400 cm^{-1}), indicating formation of stable interchain hydrogen bonding between N—H and other groups in Col stabilizing the helical structure.^{65,67} It is also well

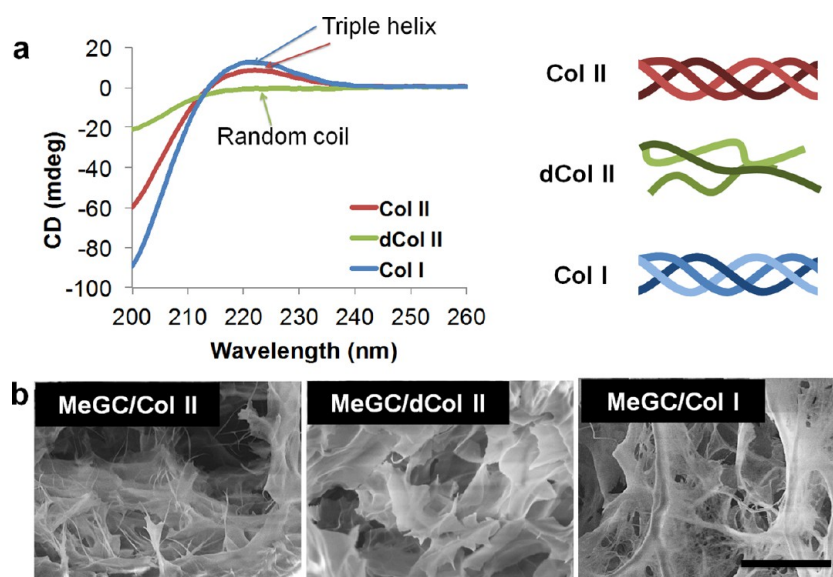


Figure 7. Conformational change of Col. (a) CD spectra of Col I, Col II, and dCol II to verify the conformation. (b) Interior morphology of MeGC/Col I, MeGC/Col II, and MeGC/dCol II investigated by SEM. Final concentrations of the different Col in hydrogels are fixed to 0.4% w/v. Scale bar is 20 μm .

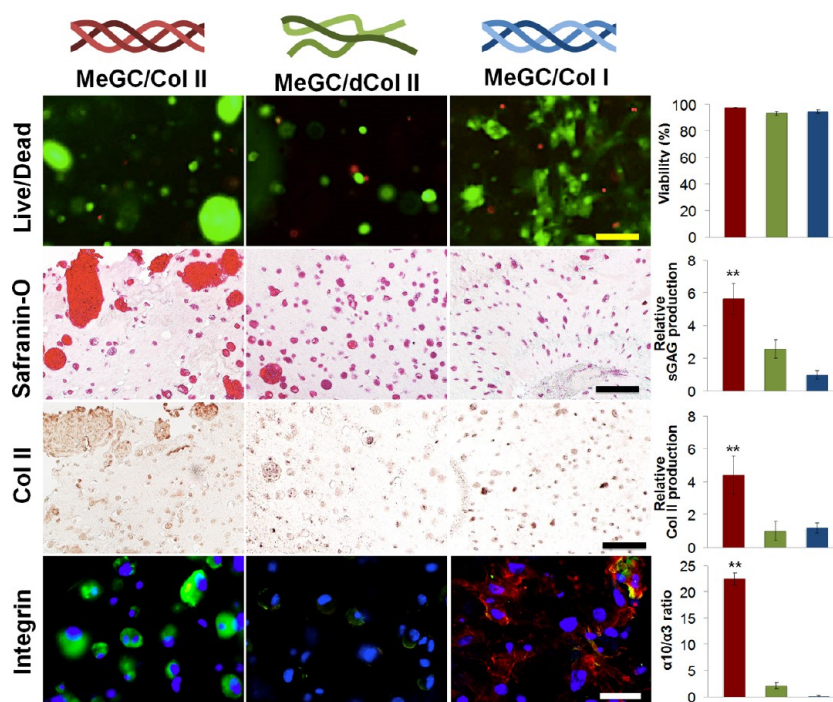


Figure 8. ADSC 3D culture in MeGC/Col hydrogels. ADSC viability in hydrogels after 3 weeks in culture analyzed by Live (green)/Dead (red) staining. Scale bar is 100 μm . Accumulated sGAG or Col II was evaluated by safranin-O staining (sGAG: orange red) or immunohistochemistry (Col II: brown), respectively, after 3 weeks in culture. Scale bar is 100 μm . Expression of integrin $\alpha 3$ (red) and $\alpha 10$ (green) subunits from ADSCs after 24 h being seeded in hydrogels. Cell nuclei: DAPI blue. Scale bar is 50 μm . Every image was quantified using ImageJ for viability (%), relative sGAG production, relative Col II production, and $\alpha 10/\alpha 3$ ratio (** $p < 0.01$ compared with other groups). Relative production of sGAG or Col II in each hydrogel was normalized to that in MeGC/Col I. MeGC/Col II, red; MeGC/dCol II, green; MeGC/Col I, blue.

demonstrated that the ratios of absorbance at 1235 cm^{-1} (amide III) to 1450 cm^{-1} (pyrrolidine ring) are around 1.0 and 0.5 for native Col and denatured Col, respectively.^{64–66} The ratio value was around 0.9 for MeGC/Col II, indicating that the triple helical structure of Col II was preserved in the MeGC/Col II hydrogel. SEM revealed the presence of nanofibrous structures in both MeGC/Col I and MeGC/Col II hydrogels, but not in MeGC/dCol II (Figure 7b).

3.8. Viability and Chondrogenic Differentiation of ADSCs in Hydrogels.

We further cultured ADSCs in hydrogels containing Col II, dCol II, and Col I for 3 weeks (Figure 8). Encapsulated ADSCs showed over 95% viability in all hydrogel systems. As expected, ADSCs in MeGC/Col II formed aggregates with 2.2-fold higher sGAG accumulation compared with MeGC/dCol II, whereas most of the encapsulated cells in MeGC/dCol II were present as individual

round cells with few aggregates, indicating the importance of Col helical structure on chondrogenesis. Although Col I possesses a triple helical structure, ADSCs encapsulated in MeGC/Col I remained as individual cells with a spindle-like shape and showed 5.7-fold lower sGAG accumulation compared with MeGC/Col II. In addition, Col II deposition was observed within the aggregates, confirming the chondrocytic phenotype of cells in the hydrogels, and Col II accumulation was significantly higher in MeGC/Col II than in MeGC/dCol II or MeGC/Col I. No significant hydrogel contraction was observed for cell encapsulating hydrogels containing Col II, whereas Col I-incorporated groups showed distinct gel contraction over culture.

3.9. Integrin Expression. Cells attach to Col through interaction of cell surface integrins with Col. Integrins $\alpha1\beta1$, $\alpha2\beta1$, and $\alpha3\beta1$ are the main receptors for Col I, and $\alpha1\beta1$, $\alpha2\beta1$, and $\alpha10\beta1$ integrins are the main receptors for Col II.¹² We evaluated expression of various integrins on ADSCs encapsulated in hydrogels (Figure 8). Strong expression of integrin $\alpha10$ was observed in ADSCs encapsulated within MeGC/Col II, but was minimally expressed in MeGC/Col I and MeGC/dCol II. In contrast, strong expression of integrin $\alpha3$ was observed in MeGC/Col I. Specifically, the ratios of expression of integrin $\alpha10$ to $\alpha3$ ($\alpha10/\alpha3$) in MeGC/Col II, MeGC/dCol II, and MeGC/Col I were 22.5, 2.1, and 0.02, respectively. These results suggest that integrin $\alpha10$ is the major Col II-binding integrin during chondrogenic differentiation and the recognition of Col II by cells was dependent on the presence of the triple helical conformation. These results correlated well with previous studies that suggested $\alpha10\beta1$ -Col II interaction is the most probable molecular interaction responsible for maintaining the chondrocyte phenotype.¹²

In this study, we have developed a simple and rapid method to stabilize natural cues of Col II or CS present in the cartilage extracellular environment into VBL/RF-initiated chitosan hydrogels. These gelation systems can be rapidly prepared using a water-soluble photoinitiator that absorbs in the visible region and have several advantages over UV light-initiated polymerizations. Exposure to visible light is less thermogenic, causes less damage to encapsulated cells, and has deeper tissue penetration.^{68,69} Our VBL/RF-initiated system showed a faster polymerization rate compared with other UV-initiated hydrogel systems using lithium acylphosphinate or Irgacure 2959 as initiators.^{37–39}

Recent cell-based therapies are attractive options to repair damaged cartilage. There is an increasing interest in developing biomaterial systems to localize precursor cells in the defective area and promote their chondrogenic differentiation. Large and complex cartilage defects are often found in chronic osteoarthritis lesions. Our hydrogel system may serve as an appropriate delivery modality for living cells and therapeutic agents to the site of extensive cartilage damage to improve clinical cartilage repair.

4. CONCLUSION

In this study, we have examined injectable and VBL-inducible chitosan hydrogel systems bearing cartilaginous ECM. These hydrogels supported proliferation and cartilage matrix production by encapsulated chondrocytes and MSCs. Incorporation of native cartilage ECM, specifically Col II, in the chitosan matrix, greatly enhanced cellular condensation, chondroid cluster formation, and chondrogenesis, which can lead to enhanced cell–matrix interaction mostly through

integrin $\alpha10\beta1$ -Col II interaction. Furthermore, chondrogenesis was affected by matrix specificity and conformation. Our findings demonstrate that Col II hydrogels enhanced by chitosan have a high potential for an injectable scaffolding system for cartilage repair. These results suggest that the strategy of incorporating the appropriate natural ECM components within a cross-linked chitosan network is a valuable means to create a specific microenvironment tailored to promote tissue regeneration.

■ ASSOCIATED CONTENT

Supporting Information

Release of Col II or CS from hydrogels, immunohistochemical staining of Col I and Col X, and FTIR spectra of Col II, MeGC/Col II, and MeGC. This material is available free of charge via the Internet at <http://pubs.acs.org>.

■ AUTHOR INFORMATION

Corresponding Author

*M. Lee. E-mail: leemin@ucla.edu.

Notes

The authors declare no competing financial interest.

■ ACKNOWLEDGMENTS

This work was supported by the UCLA Academic Senate Research Award and UCLA School of Dentistry Faculty seed grant.

■ REFERENCES

- (1) Mankin, H. J. The Response of Articular Cartilage to Mechanical Injury. *J. Bone Jt. Surg., Am. Vol.* **1982**, *64*, 460–466.
- (2) Freed, L. E.; Grande, D. A.; Lingbin, Z.; Emmanuel, J.; Marquis, J. C.; Langer, R. Joint Resurfacing Using Allograft Chondrocytes and Synthetic Biodegradable Polymer Scaffolds. *J. Biomed. Mater. Res.* **1994**, *28*, 891–899.
- (3) Spiller, K. L.; Maher, S. A.; Lowman, A. M. Hydrogels for the Repair of Articular Cartilage Defects. *Tissue Eng., Part B* **2011**, *17*, 281–299.
- (4) Mow, V. C.; Guo, X. E. Mechano-Electrochemical Properties of Articular Cartilage: Their Inhomogeneities and Anisotropies. *Annu. Rev. Biomed. Eng.* **2002**, *4*, 175–209.
- (5) Buckwalter, J. A.; Mankin, H. J. Articular Cartilage: Tissue Design and Chondrocyte-Matrix Interactions. *Instr. Course Lect.* **1998**, *47*, 477–486.
- (6) Van Vlierberghe, S.; Dubruel, P.; Schacht, E. Biopolymer-based Hydrogels as Scaffolds for Tissue Engineering Applications: A Review. *Biomacromolecules* **2011**, *12*, 1387–1408.
- (7) Loparic, M.; Wirz, D.; Daniels, A. U.; Raiteri, R.; Vanlandingham, M. R.; Guex, G.; Martin, I.; Aebi, U.; Stolz, M. Micro- and Nanomechanical Analysis of Articular Cartilage by Indentation-Type Atomic Force Microscopy: Validation with a Gel-Microfiber Composite. *Biophys. J.* **2010**, *98*, 2731–2740.
- (8) Huber, M.; Trattning, S.; Lintner, F. Anatomy, Biochemistry, and Physiology of Articular Cartilage. *Invest. Radiol.* **2000**, *35*, 573–580.
- (9) Bosnakovski, D.; Mizuno, M.; Kim, G.; Takagi, S.; Okumura, M.; Fujinaga, T. Chondrogenic Differentiation of Bovine Bone Marrow Mesenchymal Stem Cells (MSCs) in Different Hydrogels: Influence of Collagen Type II Extracellular Matrix on MSC Chondrogenesis. *Biotechnol. Bioeng.* **2006**, *93*, 1152–1163.
- (10) Sechriest, V. F.; Miao, Y. J.; Niyibizi, C.; Westerhausen-Larson, A.; Matthew, H. W.; Evans, C. H.; Fu, F. H.; Suh, J. K. GAG-Augmented Polysaccharide Hydrogel: A Novel Biocompatible and Biodegradable Material to Support Chondrogenesis. *J. Biomed. Mater. Res.* **2000**, *49*, 534–541.
- (11) Chang, K. Y.; Hung, L. H.; Chu, I. M.; Ko, C. S.; Lee, Y. D. The Application of Type II Collagen and Chondroitin Sulfate Grafted PCL

Porous Scaffold in Cartilage Tissue Engineering. *J. Biomed. Mater. Res., Part A* **2010**, *92A*, 712–723.

(12) Lu, Z.; Doulabi, B. Z.; Huang, C.; Bank, R. A.; Helder, M. N. Collagen Type II Enhances Chondrogenesis in Adipose Tissue-Derived Stem Cells by Affecting Cell Shape. *Tissue Eng., Part A* **2010**, *16*, 81–90.

(13) Vickers, S. M.; Squitieri, L. S.; Spector, M. Effects of Cross-Linking Type II Collagen-GAG Scaffolds on Chondrogenesis in Vitro: Dynamic Pore Reduction Promotes Cartilage Formation. *Tissue Eng.* **2006**, *12*, 1345–1355.

(14) Varghese, S.; Hwang, N. S.; Canver, A. C.; Theprungsirikul, P.; Lin, D. W.; Elisseeff, J. Chondroitin Sulfate based Niches for Chondrogenic Differentiation of Mesenchymal Stem Cells. *Matrix Biol.* **2008**, *27*, 12–21.

(15) Jurgens, W. J.; Lu, Z.; Zandieh-Doulabi, B.; Kuik, D. J.; Ritt, M. J.; Helder, M. N. Hyperosmolarity and Hypoxia Induce Chondrogenesis of Adipose-Derived Stem Cells in a Collagen Type 2 Hydrogel. *J. Tissue Eng. Regen. Med.* **2012**, *6*, 570–578.

(16) Yu, S. M.; Li, Y.; Kim, D. Collagen Mimetic Peptides: Progress towards Functional Applications. *Soft Matter* **2011**, *7*, 7927–7938.

(17) Vernon, R. B.; Sage, E. H. Contraction of Fibrillar Type I Collagen by Endothelial Cells: A Study in Vitro. *J. Cell. Biochem.* **1996**, *60*, 185–197.

(18) Sun, J.; Xiao, W. Q.; Tang, Y. J.; Li, K. F.; Fan, H. S. Biomimetic Interpenetrating Polymer Network Hydrogels Based on Methacrylated Alginate and Collagen for 3D Pre-Osteoblast Spreading and Osteogenic Differentiation. *Soft Matter* **2012**, *8*, 2398–2404.

(19) Gough, J. E.; Scotchford, C. A.; Downes, S. Cytotoxicity of Glutaraldehyde Crosslinked Collagen/Poly(vinyl alcohol) Films Is by the Mechanism of Apoptosis. *J. Biomed. Mater. Res.* **2002**, *61*, 121–130.

(20) van Luyn, M. J. A.; v. W, P. B.; Olde Damink, L.; Dijkstra, P. J.; Feijen, J.; Nieuwenhuis, P. Relations between in Vitro Cytotoxicity and Crosslinked Dermal Sheep Collagens. *J. Biomed. Mater. Res.* **1992**, *26*, 1091–1110.

(21) Hu, J.; Hou, Y.; Park, H.; Choi, B.; Hou, S.; Chung, A.; Lee, M. Visible Light Crosslinkable Chitosan Hydrogels for Tissue Engineering. *Acta Biomater.* **2012**, *8*, 1730–1738.

(22) Berger, J.; Reist, M.; Mayer, J. M.; Felt, O.; Peppas, N. A.; Gurny, R. Structure and Interactions in Covalently and Ionically Crosslinked Chitosan Hydrogels for Biomedical Applications. *Eur. J. Pharm. Biopharm.* **2004**, *57*, 19–34.

(23) Di Martino, A.; Sittinger, M.; Risbud, M. V. Chitosan: A Versatile Biopolymer for Orthopaedic Tissue-Engineering. *Biomaterials* **2005**, *26*, 5983–5990.

(24) Suh, J. K. F.; Matthew, H. W. T. Application of Chitosan-based Polysaccharide Biomaterials in Cartilage Tissue Engineering: A Review. *Biomaterials* **2000**, *21*, 2589–2598.

(25) Amsden, B. G.; Sukarto, A.; Knight, D. K.; Shapka, S. N. Methacrylated Glycol Chitosan as a Photopolymerizable Biomaterial. *Biomacromolecules* **2007**, *8*, 3758–3766.

(26) Tan, H. P.; Chu, C. R.; Payne, K. A.; Marra, K. G. Injectable in situ Forming Biodegradable Chitosan-Hyaluronic Acid based Hydrogels for Cartilage Tissue Engineering. *Biomaterials* **2009**, *30*, 2499–2506.

(27) Jin, R.; Moreira Teixeira, L. S.; Dijkstra, P. J.; Karperien, M.; van Blitterswijk, C. A.; Zhong, Z. Y.; Feijen, J. Injectable Chitosan-based Hydrogels for Cartilage Tissue Engineering. *Biomaterials* **2009**, *30*, 2544–2551.

(28) Moura, M. J.; Faneca, H.; Lima, M. P.; Gil, M. H.; Figueiredo, M. M. In Situ Forming Chitosan Hydrogels Prepared via Ionic/Covalent Co-Cross-Linking. *Biomacromolecules* **2011**, *12*, 3275–3284.

(29) Park, H.; Choi, B.; Hu, J.; Lee, M. Injectable Chitosan Hyaluronic Acid Hydrogels for Cartilage Tissue Engineering. *Acta Biomater.* **2013**, *9*, 4779–4786.

(30) Greenwald, R. A.; Josephson, A. S.; Diamond, H. S.; Tsang, A. Human Cartilage Lysozyme. *J. Clin. Invest.* **1972**, *51*, 2264–2270.

(31) Correia, C. R.; Moreira-Teixeira, L. S.; Moroni, L.; Reis, R. L.; van Blitterswijk, C. A.; Karperien, M.; Mano, J. F. Chitosan Scaffolds

Containing Hyaluronic Acid for Cartilage Tissue Engineering. *Tissue Eng., Part C* **2011**, *17*, 717–730.

(32) Lee, M.; Siu, R. K.; Ting, K.; Wu, B. M. Effect of Nell-1 Delivery on Chondrocyte Proliferation and Cartilaginous Extracellular Matrix Deposition. *Tissue Eng., Part A* **2010**, *16*, 1791–1800.

(33) Fan, J. B.; Park, H.; Tan, S.; Lee, M. Enhanced Osteogenesis of Adipose Derived Stem Cells with Noggin Suppression and Delivery of BMP-2. *PLoS ONE* **2013**, *8*.

(34) Chen, C. W.; Tsai, Y. H.; Deng, W. P.; Shih, S. N.; Fang, C. L.; Burch, J. G.; Chen, W. H.; Lai, W. F. Type I and II Collagen Regulation of Chondrogenic Differentiation by Mesenchymal Progenitor Cells. *J. Orthop. Res.* **2005**, *23*, 446–453.

(35) Cui, F. Z.; Wang, Y.; Cai, Q.; Zhang, W. Conformation Change of Collagen during the Initial Stage of Biomineralization of Calcium Phosphate. *J. Mater. Chem.* **2008**, *18*, 3835–3845.

(36) Jin, R.; Hiemstra, C.; Zhong, Z. Y.; Feijen, J. Enzyme-Mediated Fast in Situ Formation of Hydrogels from Dextran-Tyramine Conjugates. *Biomaterials* **2007**, *28*, 2791–2800.

(37) McCall, J. D.; Luoma, J. E.; Anseth, K. S. Covalently Tethered Transforming Growth Factor Beta in PEG Hydrogels Promotes Chondrogenic Differentiation of Encapsulated Human Mesenchymal Stem Cells. *Drug Delivery Transl. Res.* **2012**, *2*, 305–312.

(38) Sukarto, A.; Yu, C.; Flynn, L. E.; Amsden, B. G. Co-Delivery of Adipose-Derived Stem Cells and Growth Factor-Loaded Microspheres in RGD-Grafted N-Methacrylate Glycol Chitosan Gels for Focal Chondral Repair. *Biomacromolecules* **2012**, *13*, 2490–2502.

(39) Villanueva, I.; Gladem, S. K.; Kessler, J.; Bryant, S. J. Dynamic Loading Stimulates Chondrocyte Biosynthesis When Encapsulated in Charged Hydrogels Prepared from Poly(ethylene glycol) and Chondroitin Sulfate. *Matrix Biol.* **2010**, *29*, 51–62.

(40) DeKosky, B. J.; Dorner, N. H.; Ingavle, G. C.; Roatch, C. H.; Lomakin, J.; Detamore, M. S.; Gehrke, S. H. Hierarchically Designed Agarose and Poly(ethylene glycol) Interpenetrating Network Hydrogels for Cartilage Tissue Engineering. *Tissue Eng., Part C* **2010**, *16*, 1533–1542.

(41) Brigham, M. D.; Bick, A.; Lo, E.; Bendali, A.; Burdick, J. A.; Khademhosseini, A. Mechanically Robust and Bioadhesive Collagen and Photocrosslinkable Hyaluronic Acid Semi-Interpenetrating Networks. *Tissue Eng., Part A* **2009**, *15*, 1645–1653.

(42) Ala-Kokko, L.; Baldwin, C. T.; Moskowitz, R. W.; Prockop, D. J. Single Base Mutation in the Type II Procollagen Gene (COL2A1) as a Cause of Primary Osteoarthritis Associated with a Mild Chondrodysplasia. *Proc. Natl. Acad. Sci. U. S. A.* **1990**, *87*, 6565–6568.

(43) Burgeson, R. E.; Hollister, D. W. Collagen Heterogeneity in Human Cartilage: Identification of Several New Collagen Chains. *Biochem. Biophys. Res. Commun.* **1979**, *87*, 1124–1131.

(44) Tamura, H.; Tsuruta, Y.; Tokura, S. Preparation of Chitosan-Coated Alginate Filament. *Mater. Sci. Eng., C* **2002**, *20*, 143–147.

(45) Shepherd, D. E.; Seedhom, B. B. The “Instantaneous” Compressive Modulus of Human Articular Cartilage in Joints of the Lower Limb. *Rheumatology* **1999**, *38*, 124–132.

(46) Temel, A.; Kazokoglu, H.; Taga, Y. Tear Lysozyme Levels in Contact Lens Wearers. *Ann. Ophthalmol.* **1991**, *23*, 191–194.

(47) Hankiewicz, J.; Swierczek, E. Lysozyme in Human Body Fluids. *Clin. Chim. Acta* **1974**, *57*, 205–209.

(48) Porstmann, B.; Jung, K.; Schmechta, H.; Evers, U.; Pergande, M.; Porstmann, T.; Kramm, H. J.; Krause, H. Measurement of Lysozyme in Human Body Fluids: Comparison of Various Enzyme Immunoassay Techniques and Their Diagnostic Application. *Clin. Biochem.* **1989**, *22*, 349–355.

(49) Bueno, E. M.; Bilgen, B.; Carrier, R. L.; Barabino, G. A. Increased Rate of Chondrocyte Aggregation in A Wavy-Walled Bioreactor. *Biotechnol. Bioeng.* **2004**, *88*, 767–777.

(50) Vickers, S. M.; Gotterbarm, T.; Spector, M. Cross-Linking Affects Cellular Condensation and Chondrogenesis in Type II Collagen-GAG Scaffolds Seeded with Bone Marrow-Derived Mesenchymal Stem Cells. *J. Orthop. Res.* **2010**, *28*, 1184–1192.

(51) Park, H.; Temenoff, J. S.; Tabata, Y.; Caplan, A. I.; Raphael, R. M.; Jansen, J. A.; Mikos, A. G. Effect of Dual Growth Factor Delivery

on Chondrogenic Differentiation of Rabbit Marrow Mesenchymal Stem Cells Encapsulated in Injectable Hydrogel Composites. *J. Biomed. Mater. Res., Part A* **2009**, *88*, 889–897.

(52) Zhang, C.; Sangaj, N.; Hwang, Y.; Phadke, A.; Chang, C.-W.; Varghese, S. Oligo(trimethylene carbonate)–Poly(ethylene glycol)–Oligo(trimethylene carbonate) Triblock-based Hydrogels for Cartilage Tissue Engineering. *Acta Biomater.* **2011**, *7*, 3362–3369.

(53) Chang, C. H.; Liu, H. C.; Lin, C. C.; Chou, C. H.; Lin, F. H. Gelatin-Chondroitin-Hyaluronan Tri-Copolymer Scaffold for Cartilage Tissue Engineering. *Biomaterials* **2003**, *24*, 4853–4858.

(54) Bian, L.; Angione, S. L.; Ng, K. W.; Lima, E. G.; Williams, D. Y.; Mao, D. Q.; Ateshian, G. A.; Hung, C. T. Influence of Decreasing Nutrient Path Length on the Development of Engineered Cartilage. *Osteoarthritis Cartilage* **2009**, *17*, 677–685.

(55) Kelly, T. A.; Ng, K. W.; Wang, C. C.; Ateshian, G. A.; Hung, C. T. Spatial and Temporal Development of Chondrocyte-Seeded Agarose Constructs in Free-Swelling and Dynamically Loaded Cultures. *J. Biomech.* **2006**, *39*, 1489–1497.

(56) Bian, L.; Zhai, D. Y.; Zhang, E. C.; Mauck, R. L.; Burdick, J. A. Dynamic Compressive Loading Enhances Cartilage Matrix Synthesis and Distribution and Suppresses Hypertrophy in hMSC-Laden Hyaluronic Acid Hydrogels. *Tissue Eng., Part A* **2012**, *18*, 715–724.

(57) Lee, M.; Dunn, J. C.; Wu, B. M. Scaffold Fabrication by Indirect Three-Dimensional Printing. *Biomaterials* **2005**, *26*, 4281–4289.

(58) Lee, M.; Wu, B. M.; Dunn, J. C. Effect of Scaffold Architecture and Pore Size on Smooth Muscle Cell Growth. *J. Biomed. Mater. Res., Part A* **2008**, *87*, 1010–1016.

(59) Ishaug-Riley, S. L.; Crane-Kruger, G. M.; Yaszemski, M. J.; Mikos, A. G. Three-Dimensional Culture of Rat Calvarial Osteoblasts in Porous Biodegradable Polymers. *Biomaterials* **1998**, *19*, 1405–1412.

(60) Ling, Y.; Rubin, J.; Deng, Y.; Huang, C.; Demirci, U.; Karp, J. M.; Khademhosseini, A. A Cell-Laden Microfluidic Hydrogel. *Lab Chip* **2007**, *7*, 756–762.

(61) Geckil, H.; Xu, F.; Zhang, X.; Moon, S.; Demirci, U. Engineering Hydrogels as Extracellular Matrix Mimics. *Nanomedicine* **2010**, *5*, 469–484.

(62) Toh, W. S.; Lim, T. C.; Kurisawa, M.; Spector, M. Modulation of Mesenchymal Stem Cell Chondrogenesis in a Tunable Hyaluronic Acid Hydrogel Microenvironment. *Biomaterials* **2012**, *33*, 3835–3845.

(63) Lin, C. C.; Sawicki, S. M.; Metters, A. T. Free-Radical-Mediated Protein Inactivation and Recovery during Protein Photoencapsulation. *Biomacromolecules* **2008**, *9*, 75–83.

(64) Mitra, T.; Sailakshmi, G.; Gnanamani, A.; Mandal, A. B. Studies on Cross-Linking of Succinic Acid with Chitosan/Collagen. *Mater. Res.* **2013**, *16*, 755–765.

(65) Li, H.; Liu, B. L.; Gao, L. Z.; Chen, H. L. Studies on Bullfrog Skin Collagen. *Food Chem.* **2004**, *84*, 65–69.

(66) Sader, M. S.; Martins, V. C.; Gomez, S.; LeGeros, R. Z.; Soares, G. A. Production and in vitro Characterization of 3D Porous Scaffolds Made of Magnesium Carbonate Apatite (MCA)/Anionic Collagen Using a Biomimetic Approach. *Mater. Sci. Eng., C* **2013**, *33*, 4188–4196.

(67) Cao, H.; Xu, S.-Y. Purification and Characterization of Type II Collagen from Chick Sternal Cartilage. *Food Chem.* **2008**, *108*, 439–445.

(68) Elisseeff, J.; Anseth, K.; Sims, D.; McIntosh, W.; Randolph, M.; Langer, R. Transdermal Photopolymerization for Minimally Invasive Implantation. *Proc. Natl. Acad. Sci. U. S. A.* **1999**, *96*, 3104–3107.

(69) Sowa, P.; Rutkowska-Talipska, J.; Rutkowski, K.; Kosztyla-Hojna, B.; Rutkowski, R. Optical Radiation in Modern Medicine. *Postepy Dermatol. Alergol.* **2013**, *30*, 246–251.